Review of methods for intraoperative margin detection for breast conserving surgery

Benjamin W. Maloney
David M. McClatchy
Brian W. Pogue
Keith D. Paulsen
Wendy A. Wells
Richard J. Barth, Jr.

SPIE.

Review of methods for intraoperative margin detection for breast conserving surgery

Benjamin W. Maloney,[a,]* David M. McClatchy,[a] Brian W. Pogue,[a,b,c] Keith D. Paulsen,[a,b,c] Wendy A. Wells,[c,d] and Richard J. Barth Jr.[b,c]

[a]Dartmouth College, Thayer School of Engineering, Hanover, New Hampshire, United States
[b]Geisel School of Medicine, Department of Surgery, Hanover, New Hampshire, United States
[c]Norris Cotton Cancer Center, Dartmouth-Hitchcock Medical Center, Lebanon, New Hampshire, United States
[d]Geisel School of Medicine, Department of Pathology and Laboratory Medicine, Hanover, New Hampshire, United States

Abstract. Breast conserving surgery (BCS) is an effective treatment for early-stage cancers as long as the margins of the resected tissue are free of disease according to consensus guidelines for patient management. However, 15% to 35% of patients undergo a second surgery since malignant cells are found close to or at the margins of the original resection specimen. This review highlights imaging approaches being investigated to reduce the rate of positive margins, and they are reviewed with the assumption that a new system would need high sensitivity near 95% and specificity near 85%. The problem appears to be twofold. The first is for complete, fast surface scanning for cellular, structural, and/or molecular features of cancer, in a lumpectomy volume, which is variable in size, but can be large, irregular, and amorphous. A second is for full, volumetric imaging of the specimen at high spatial resolution, to better guide internal radiologic decision-making about the spiculations and duct tracks, which may inform that surfaces are involved. These two demands are not easily solved by a single tool. Optical methods that scan large surfaces quickly are needed with cellular/molecular sensitivity to solve the first problem, but volumetric imaging with high spatial resolution for soft tissues is largely outside of the optical realm and requires x-ray, micro-CT, or magnetic resonance imaging if they can be achieved efficiently. In summary, it appears that a combination of systems into hybrid platforms may be the optimal solution for these two very different problems. This concept must be cost-effective, image specimens within minutes and be coupled to decision-making tools that help a surgeon without adding to the procedure. The potential for optical systems to be involved in this problem is emerging and clinical trials are underway in several of these technologies to see if they could reduce positive margin rates in BCS. © *2018 Society of Photo-Optical Instrumentation Engineers (SPIE)* [DOI: 10.1117/1.JBO.23.10.100901]

Keywords: breast conserving surgery; optical; imaging; lumpectomy; spectroscopy; breast cancer; mammography.

Paper 180466VR received Jul. 23, 2018; accepted for publication Oct. 3, 2018; published online Oct. 27, 2018.

1 Introduction

Technologies currently available for breast imaging offer high sensitivity and specificity, but they have been developed largely for the tasks of screening and presurgical planning. The most common clinical modality for breast imaging is x-ray mammography, which has an estimated sensitivity of between 83% and 95% and an estimated specificity of between 90% and 98%.[1] In comparison, imaging tools for inspection of surgical cavities or resected specimens are much less well developed. In this paper, technologies for detection and imaging of surgical specimens are reviewed in order to highlight clinical needs and potential value in terms of breast cancer management.

Breast malignancy is the second most prevalent cancer diagnosis for women in the United States with 1 out of every 8 women being diagnosed with the disease during a lifetime. In the United States, nearly 250,000 new cases are diagnosed each year and more than 40,000 women will die from breast cancer annually.[2] The recommended treatment for early-stage disease is breast conserving surgery (BCS). This procedure seeks to remove the cancer with a margin of normal tissue surrounding the resected specimen. In many cases, BCS is followed by chemotherapy and/or radiotherapy. Long-term outcomes of BCS are equivalent to mastectomy for early stage breast cancers if clear margins are obtained during the process.[3]

Current consensus guidelines define a surgical margin as negative if no malignant cells are observed at the surface of the resected specimen for invasive cancers.[4] The judgement of "no tumor on ink" is used to indicate that the inked borders are free from any detectable tumor tissue. For ductal carcinoma *in situ* (DCIS), a clear margin of 2 mm is now recommended.[5] About 20% to 40% of BCS procedures result in margins, which are either positive or close to having cancer on the surface of the tissue and require a second operation to remove more tissue.[6–9] The high percentage of re-excisions leads to additional costs, additional anxiety for patients, and an increased risk of postsurgical complications (e.g., infection). Thus improved imaging tools are needed to ensure clear margins at the time of BCS; and hence, the motivation to review state-of-the-art intrasurgical tools for margin assessment during BCS. Although other studies have reviewed the literature of margin management in BCS, the focus has been more around the surgical procedure choices rather than the imaging technologies possible.[10,11] This review focuses on the latter issue of what technologies would be optimal for the problem.

Ideally, a system to improve positive margin detection would have an extremely high sensitivity in order to accurately detect

*Address all correspondence to: Benjamin W. Maloney, E-mail: benjamin.w.maloney.th@dartmouth.edu
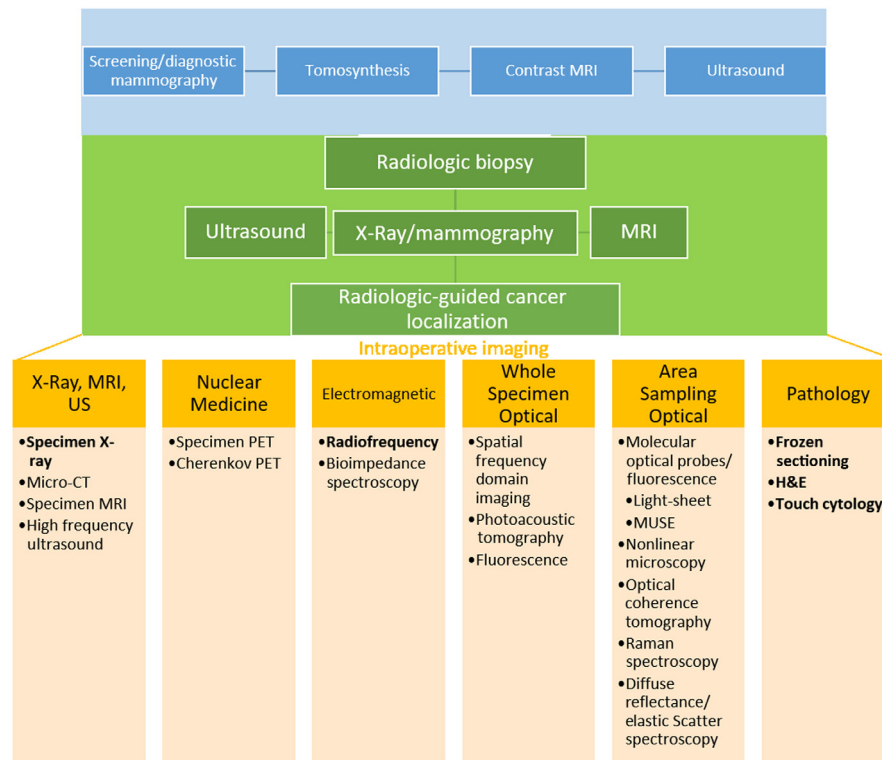
Fig. 1 Imaging as part of breast cancer surveillance/diagnosis (blue) and therapy (green) is illustrated. Intraoperative imaging tools (yellow), which have been attempted for margin assessment in BCS, are discussed.

all tumor found in the margins, with a sensitivity of above 95%. Specificity would be less important, because detection is the primary concern in this setting, but excess false positive detection would ultimately be detrimental to the system and its use, and so it is likely needed to be about 85% in an ideal situation. An alternative view though is that current practice of a surgeon making the decision where to end the resection has a specificity of about 65% to 85%, based upon the recall rate from BCS surgery (35% to 15% depending upon the center), and so a system should have a specificity at least matching the best practices today, at 85%.[12–15]

Figure 1 shows a conceptual flowchart, indicating where imaging is involved in breast healthcare, with screening methods appearing at the top in blue, and invasive/diagnostic methods in green. The range of imaging/detection tools for intrasurgical use appears in yellow and is categorized by technology subtype. This part of the figure summarizes a number of different forms of imaging, in which studies involving human specimens from BCS have been reported. Each of these methods is discussed in detail. Methods appearing in bold font are either FDA approved for margin detection in BCS or are part of standard-of-care during surgery. This figure conveys the general workflow of imaging for breast cancer beginning with surveillance via screening mammography followed by diagnostic workup (in blue) when imaging abnormalities are found leading to surgical planning (green) and intraoperative imaging (in yellow) once a definitive cancer diagnosis occurs and BCS is chosen for treatment.

2 Preoperative Imaging

Although this review focuses on imaging techniques used intraoperatively, the other major uses of imaging in, and leading up

to, BCS are summarized. Clearly, the most widely accepted imaging tool for breast cancer screening is x-ray mammography because of the legislated and clinically prescribed screening programs currently in place that have contributed to reduced mortality rates of the disease. Annual screening is recommended for women aged 50 to 74 and sometimes for women in the age range 40 to 49 based on patient history, although the guideline is subject to debate,[16] individual differences (e.g., family history) often come into play.[17] Screening mammography involves low-energy x-ray projections to image the compressed breast and resulting data are read by a radiologist for local abnormalities.[18] In some geographic locations and for certain groups of women, x-ray tomosynthesis may be used instead to create quasi-3-D or multiple 2-D views that mitigate the reading challenges presented by tissue overlap, which can be especially difficult in dense breast tissue.[19] Additionally, women with dense breasts are offered 3-D ultrasound screening in some locations, to ensure that the process is as sensitive as possible at finding abnormalities.[20,21] For women with a strong familiar disposition or other high-risk factors, magnetic resonance imaging (MRI) is the preferred screening tool.[22,23]

If an abnormality is found, diagnostic workup and biopsy may occur to determine the origin of the tissue and provide a definitive diagnosis. Diagnostic workup often includes additional mammography at higher dose but with superior clarity, spot x-ray mammograms, 3-D tomosynthesis, 3-D or 2-D ultrasound, and/or contrast-enhanced MRI. Selections from these methods depend on findings from previous tests and the patient's data.[24–26] Each of these methods may be used to guide biopsy or occur during a subsequent biopsy procedure to obtain tissue for pathology processing. Pathological diagnosis

is performed on formalin-fixed and stained tissues, with optional FISH and immunohistochemical stain readings.

Imaging is also used for BCS planning. Examples include radiological biopsies, presurgical CT, x-ray-guided wire placement and localization, ultrasound for tumor localization, and other forms of tumor localization such as use of radioactive seeds.[27–30]

3 Intraoperative Imaging

3.1 Histology

Histology methods for margin detection assess the microscopic cellular structure of tissue. These approaches are slower than other imaging techniques and are usually more labor intensive. They are also the most well established and currently serve as the gold standard for comparisons with other detection approaches.

The current gold standard for margin classification is provided by a surgical pathologist, after surgery. Tissue is fixed, processed, sectioned, stained with hematoxylin and eosin (H&E), and interpreted microscopically. Although the approach is accurate, it is also time consuming and is completed over several days after the original surgery, depending on the specimen size and diagnostic complexity. If positive or close margins are found, then a second surgical procedure may need to be performed. This outcome leads to additional stress for the patient, costs to healthcare system, potentially suboptimal cosmesis and increased risk of surgical infection from the re-excision.

3.1.1 Frozen sectioning

Frozen sectioning is the most commonly used method for intraoperative margin assessment during BCS and is considered standard-of-care in some hospitals.[31] Frozen section analysis consists of freezing small pieces of tissue, then sectioning, staining, and interpreting them under a microscope. The time from the tissue leaving the operating room (OR) and a microscopic diagnosis being rendered is 20 to 30 min, during which period the patient remains under anesthesia. Freezing tissue generates significant artifacts, especially in fatty tissues, such as the breast. It can also be damaging such that tissue used for frozen sectioning may not be viable for the routine histopathologic margin assessment performed later. Frozen section interpretations are expensive and require additional technical staff to cut the specimens. These limitations result in a small fraction of the specimen margin being frozen and analyzed, leaving a large percentage of the tissue unassessed. Frozen sectioning was also found to be slightly less effective for DCIS and larger tumors. Frozen sectioning has been shown to reduce positive margin rates, but not eliminate them.[32–34] This technique has a sensitivity of 83% and a specificity of 95%.[35] Frozen section analysis produces information similar to that found in standard histology at a much faster rate. However, it is not the ideal solution to the margin issue in BCS due to its low sampling percentage, large technical issues, and high cost.

3.1.2 Imprint cytology

Imprint cytology is another pathology-based margin detection method used as a standard-of-care during BCS. Here each surface of a resected specimen is positioned and pressed into a slide which is then fixed and stained. The method is based on the idea that malignant cells will stick to the slides, whereas adipose cells will not adhere. It offers similar accuracy and predictive value as frozen sectioning while taking less time (about 15 rather than 30 min) and being less damaging to the tissue. Imprint cytology also examines the entire surface of the resected tissue rather than only the spot checks that occur with frozen sectioning. However, rapid and accurate interpretation requires a cytopathology-trained professional in the OR in addition to the regular surgical staff and relies on subspecialist diagnostic skills as well.[32] Varying results have also been obtained when the surface of the resected tissue has been altered by cauterization and dryness. Over interpreting atypical cells at the surface that are not malignant may also be problematic.[36] This technique has a sensitivity of 72% and a specificity of 97%.[35] Imprint cytology has strong aspects in that it samples the entire surface of the sample rapidly and offers similar information to standard histology. However, its low sensitivity, need for a trained cytopathologist, and various artifacts prevent it from being an ideal solution.

3.2 X-Ray Imaging

Contrast from x-ray attenuation of fibroglanduar versus adipose tissue is high, whereas differences between tumors and fibroglandular tissues are more subtle. Further, higher-keV x-rays (50 to 60 keV) offer better penetration into tissue but lower-keV x-rays (15 to 25 keV) generate superior contrast for imaging internal structures. Table 1 summarizes several x-ray imaging systems for resected specimen scanning in terms of their technical specifications (field of view, resolution, focal spot, energy range, and footprint).[37–41]

3.2.1 Radiographic imaging (projections)

Radiographic approaches exploit 2-D x-ray projections to image tissue and produce contrast based on beam attenuation through the tissue. Standard-of-care involves using these x-ray projections to guide placement of a surgical wire to localize the center of the apparent lesion and verify that the lesion appears to be contained within the specimen. A study compared intraoperative digital specimen mammography to standard specimen radiography.[42] Both methods were evaluated for tumor localization and margin estimation, although standard specimen mammography is performed outside the OR environment, so it involves removing the resected tissue from the OR and transporting it to another location to perform the imaging. The study found that digital specimen mammography produced comparable results in the OR.[42] Another study found that intraoperative digital specimen mammography did not reduce operation times compared to convention specimen mammography as one might expect but that it did lead to a significant reduction in positive margins.[43] Intraoperative x-ray imaging is done using digital mammography, which uses a solid-state detector to increase the dynamic range of the system. Beam parameters are able to be optimized for different thicknesses of breast. One study found that for smaller breasts (21- to 32-mm in thickness) a 25- or 28-kV Mo/Mo target/filter setting was found to be optimal and for breasts with thicknesses >45 mm, a 34-kV beam with Rh/Rh target/filter was ideal.[44]

Often, multiple radiographic images are acquired in orthogonal 2-D views to obtain 3-D information.[45] In a recent study, intraoperative specimen radiography yielded a sensitivity of 41% and a specificity 78% with 2-D imaging and a sensitivity of 47% and a specificity of 75% with 3-D imaging for positive margins.[46] Although the addition of specimen radiography

Table 1 Technical specifications of x-ray systems used for specimen margin analysis during BCS in published studies.[37–41] The imaging areas, spatial resolution all dramatically affect the imaging time, and so comparisons on all three of these issues is challenging. But in general imaging full specimens on a timescale near a minute or less is possible for both x-ray and micro-CT with spatial resolution near 10 to 20 μm.

System	Faxitron Biovision+	Faxitron Biovision	Hologic trident	Perkin Elmer IVIS spectrumCT	Bruker Skyscan 1173
Type	2-D x-ray/3-D x-ray with wedge	2-D x-ray/3-D x-ray with wedge	x-ray cabinet	Micro-CT	Micro-CT
Imaging area	240 × 300 mm	100 × 150 mm	120 × 140 mm	120 × 120 × 30 mm	140-mm diameter 200-mm length
Resolution	21 lp/mm (24.1 μm)	10 lp/mm (48.2 μm)	7.1 lp/mm	13.5 μm	<4 to 5 μm, 7 to 8 μm low contrast
Focal spot	10 μm nominal	50 μm	50 μm	40 to 300 μm	<5 μm
Energy	5 to 50 kV	20 to 40 kV	20 to 35 kV	Up to 50 kV	40 to 130 kV
Scan time				3.6 to 72 s	
Reconstruction time				40 to 150 s	
Footprint	53 cm × 38 cm × 170 cm	56 cm × 57 cm × 170 cm	26.5 × 37.5 × 68.3 in.	203 × 163 × 214 cm	107 × 72 × 62.5 cm

lowered the number of re-excisions, it also generated a large number of false positives that led to unnecessary tissue removal. Interestingly, only a small increase in the number of re-excisions was found if 3-D radiographic imaging was used instead of its 2-D counterpart with the Faxitron Biosystem and wedge tissue holding system.[46] Another study investigated digital breast tomosynthesis relative to digital mammography and found the former was better at identifying regions of invasive cancer, particularly in the vertical plane of the tomosynthesis data. These tomosynthesis data use x-ray projections at different angles to obtain 3-D information and create an image stack of thin slices of cross-sectional images rather than orthogonal images such as those shown earlier in this review.[47]

This type of x-ray imaging is conventionally accepted and is the same technology (mammography and tomosynthesis) used for *in vivo* breast imaging. It provides volumetric image data with good fat/tissue contrast, and therefore, is readily interpreted. The subtleties of radiological reading of these images are also well developed, and providing a radiology consult to OR personnel when needed has been worked out in most medical centers. Additionally, presurgical mammo/tomo images can be compared directly to the specimen mammo/tomo results, allowing for improved interpretation of resection accuracy. Limitations include lack of specificity for tumor versus dense fibroglandular tissue, which diminish accuracy for margin assessment.

3.2.2 *Micro-CT (3-D volumes)*

One form of radiographic projection imaging of particular interest is micro-CT. Micro-CT uses x-ray projections in the same manner as convention CT, however, it is designed to have much higher resolution in the micrometer scale. This is important since the resolution needed to confirm margin status and the shape of microcalcifications leading to the margins in resected specimens is on this spatial scale. Micro-CT has been used in several studies to image resected tumor tissues, shaved cavity margins, and auxiliary lymph nodes in BCS. Micro-CT captures x-ray projections at many angles (typically 180) to create a volumetric dataset. Accordingly, micro-CT recovers higher soft tissue contrast because of the acquisition of multiple beam angles and use of filtered back projection reconstruction. The 3-D image volume can be used to identify tumor location in resected specimens or shaved cavity margins. Micro-CT may also be useful in lymph node analysis and assessment of mastectomy specimens. Figure 2 shows an example illustrating more accurate estimation of tumor distance from the specimen edge with micro-CT relative to 2-D radiography.[48] Investigations of micro-CT as a predictor of whether breast microcalcifications indicate malignant or benign conditions at the tissue surface are underway because the approach provides 3-D shape analysis at sufficient spatial resolution. These microcalcifications can be used to determine which margins are most likely to contain a positive margin.[49,50] Micro-CT has also been combined with other types of imaging systems such as spatial frequency domain imaging (SFDI) to create multidimensional data that may offer accurate specimen margin assessments.[51] A recent study of fresh lumpectomy specimens was able to identify the correct margin status on 25 out of 29 patients that were able to be analyzed. There were four false negative results which lead to a sensitivity of 56% and a specificity of 100%.[52] Another recent study of 32 patients yielded a sensitivity of 60% and a specificity of 67%.[53]

Micro-CT generates volumetric data with reasonably high-soft tissue contrast, which is its main advantage over 2-D x-ray projection imaging. Imperfect discrimination between tumor and fibroglandular/dense tissue still occurs and limits completely accurate margin assessment of specimens. Additionally, the acquisition of multiple beam angles of data, image reconstruction, and the need to read/diagnose the volumetric 3-D results requires more time than 2-D imaging.

3.3 *Magnetic Resonance Imaging*

MRI applies high magnetic fields (0.1 to 7 Tesla) with sequenced radiofrequency signals to recover images of the
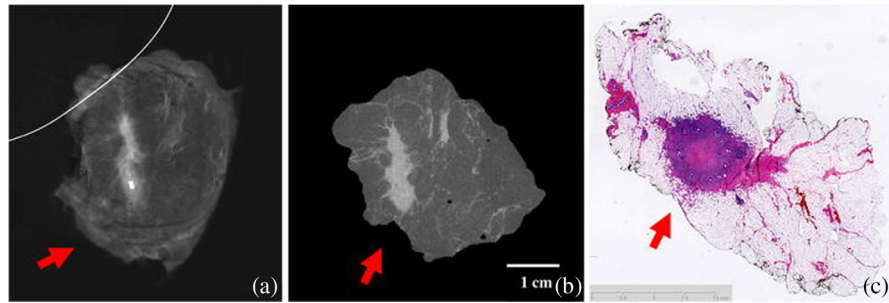
Fig. 2 (a) Tumor mass appears far from the margin in 2-D radiography. (b) Micro-CT cross section indicates tumor closer to the edge of the specimen. (c) Histopathology slide shows tumor mass closer to edge, more similar to the micro-CT slice than the 2-D radiography image.[48] The mammography images are limited to one or two views, while the micro-CT is full volumetric. The whole mount histology is useful but not routinely done for any lumpectomy specimens, so the value of a micro-CT is to visualize the tumor extent in all 3-D. Reprinted by permission from Ref. 48, Springer Nature.

tissue's nuclear magnetic dipole interactions. Soft tissue differentiation is the strongest benefit of MRI and it is more sensitive to breast cancer than x-ray imaging. One study found a sensitivity of 93% and a specificity of 65%.[54–56] MR images are acquired preoperatively with contrast injection and are used for surgical planning often to detect satellite lesions, which extend beyond the main malignancy.[57]
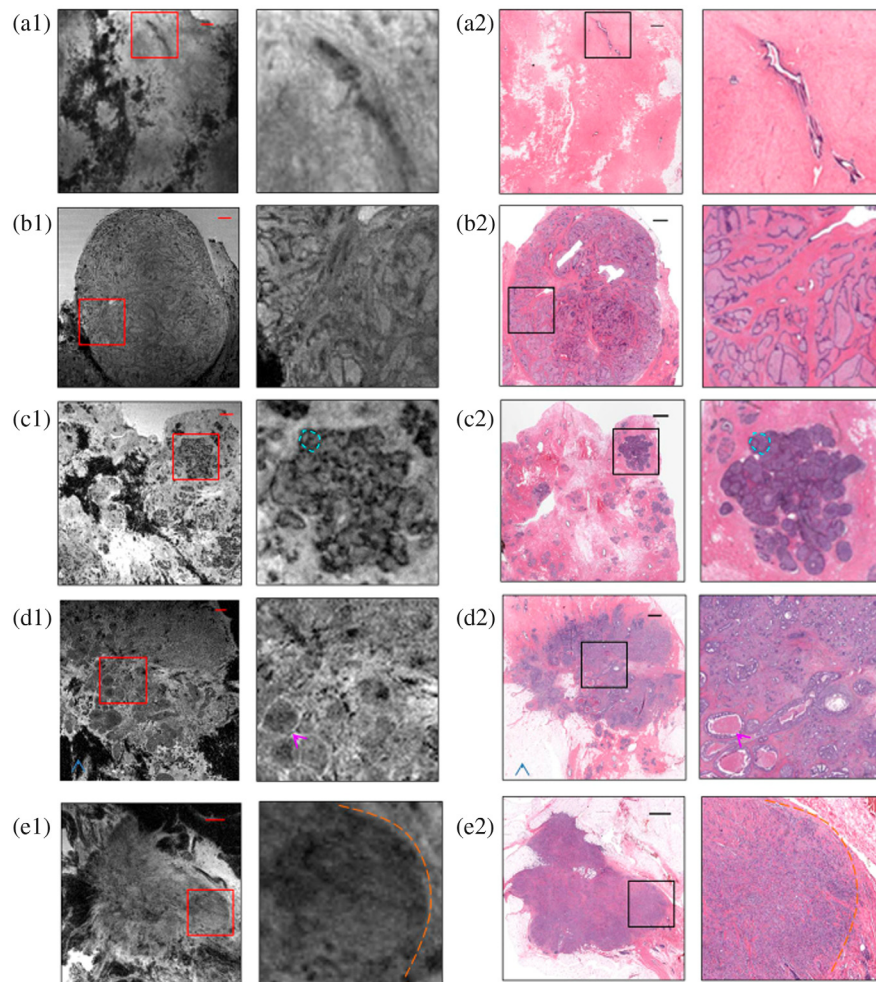
Fig. 3 MRI images (left) and the corresponding H&E slides (right). Each is followed by a magnified version of the portion of the image inside the viewing box superimposed on the lower magnification imaging data. Classifications are: (a) normal breast tissue, (b) fibroadenoma, (c) DCIS, (d) invasive ductal carcinoma and DCIS, and (e) invasive lobular carcinoma.[58] The value of MRI is the best soft tissue resolution for full volumetric imaging, with high spatial resolution, while the limitation of this has always been high cost of the systems and long scan times. Adapted from Ref. 58. Creative Commons Attribution License 4.0, Copyright 2015, Macmillan Publishers Limited.

One study of MRI applied to resected breast specimens achieved $59 \times 59 \times 94$ μm^3 spatial resolution, albeit with an imaging time exceeding hour, which is likely too long for routine surgical use. In that study, 14 pathologists provided diagnoses based on the MR images, but achieved the correct results only 36% of the time, and the accuracy of categorizing benign versus malignant lesions was only 57%. The study pathologists had no prior MR interpretation training, so their lack of experience likely affected the results negatively. Although these diagnostic performances were not very promising, study showed the feasibility of using specimen MRI, intraoperatively. Given the MR soft tissue contrast available through MRI further study is warranted in the context of specimen imaging. Figure 3 shows a number of representative cases of different breast tissue diagnoses for MR images and their corresponding H&E images.[58] The development of low-medium field, self-shielded MRI scanners, which present a lower risk, could open up the field to use in the surgical settings.[59] Another study used a high magnetic field (9.4 T) specimen MRI. This study found that for IDC, MRI is a very promising form of margin localization. It did note that for DCIS, this method was far less effective. It also noted the number of challenges that will make it difficult for MRI to be adopted into margin assessment in clinical practice including cost, ease of use, and imaging time, which are all serious concerns for margin management in BCS.[60] MRI is a common modality for other uses in hospitals so using it for breast cancer margin detection is attractive since there is likely already trained staff that knows how to interpret the images. It is also attractive since it has much better soft tissue contrast than x-ray imaging does, which is the most common intraoperative technique for lowering margin rates. However, the long scan times for MR imaging and the high cost of this technique make this a nonideal solution to lowering positive margin rates in BCS.

3.4 Ultrasound

High-frequency ultrasound imaging of the specimen margin visualizes structural features of the tissue and its associated heterogeneity. One report of ultrasound (in a range of 20 to 80 MHz) evaluated 34 samples from 17 patients and found the technique distinguished lobular carcinoma from normal tissue with specificity of 100% and sensitivity of 86%; ductal carcinoma from normal tissue with specificity of 100% and sensitivity of 74%; benign pathologies from cancer with specificity of 80% and a sensitivity of 82%; and fat necrosis from adenoma with specificity of 80% and sensitivity of 100%.[61] A more recent study of 132 patients reported a sensitivity of 44% and a specificity of 94%. This study notes that US may be a better alternative to specimen x-ray in cases of dense breasts, where x-ray has the most difficulty. It also notes how US is much faster and far less expensive than the more commonly used modality of specimen x-ray.[62] Advances in ultrasound transducers and signal processing continue to be reported; hence, the value of high-frequency ultrasound to margin assessment may increase. Improved understanding of the strengths and weaknesses of this modality in the context of specimen imaging is needed, and advances such as 3-D ultrasound currently being applied to dense breasts could be utilized for specimen scanning as well.[63] Ultrasound guidance for surgical margins provides a tool that can be useful for determining margin status in a low-cost manner, especially for women with dense breasts where other methods may not work as well.

However, the necessity of larger margins (up to 10 mm being considered positive in some studies), low-sensitivity numbers, and requirement to be scanned make it so ultrasound will likely not be a full solution to the margin status problem.

3.5 Nuclear Medicine

Nuclear imaging involves administration of radioactive tracers *in vivo*, prior to surgery, and obtains diagnostic or treatment related information, accordingly. The approach provides more functional rather than structural data since it inherently depends on blood flow delivery and biological or biophysical uptake of the agent. This type of breast imaging includes detection of positron annihilation radiation and Cherenkov optical imaging, and both have been evaluated for specimen margin assessment.

Although this review is focused on imaging of surgical margins, many of these techniques can be used to assess sentinel lymph nodes as well particularly those using nuclear medicine. The sentinel lymph node is the first drainage site for breast cancers and provides information about the metastatic status of the disease.[48,64,65]

3.6 Positron Emission Tomography

3.6.1 Customized breast PET

18F-fluorodeoxyglucose is by far the most commonly used positron emission tomography (PET) agent, and localizes tumor based on signal intensity. This signal intensity change is from the increased metabolism of tumors and the resulting increase of glucose uptake. It can also be used to check the status of margins. In one study, a preoperative positron emission tomography/computed tomography (PET/CT) scan was acquired to characterize tumor. Images guided the resection, and since the radioactive signal could be detected *ex vivo*, a gamma probe assisted in the assurance of clear margins. Then a full PET/CT scan was performed on the resected tissue to determine if the amount of tumor removed matched with the extent of disease observed on preoperative imaging. A final patient exam was also performed after the surgery to localize residual tumor, if any. In the study, 18F-fluorodeoxyglucose uptake was not specific, increasing likelihood of false positive results. The method has also been used to guide tumor localization. It is important to note that this has only shown feasibility since there were only two patients involved in this initial study.[64] Breast PET has shown a sensitivity of 92% to 96% and a specificity of 84% to 91%.[66–68] Breast PET shows promise with high sensitivity and specificity. It is also a modality commonly used in hospitals for other purposes so there likely is already staff who know how to interpret the results well. However, PET is expensive, time-consuming, and invasive which makes it an unattractive solution to the positive margin percentage problem in BCS.

3.6.2 Cherenkov PET

Another use of PET in margin status detection is Cherenkov luminescence imaging (CLI), which captures Cherenkov optical photons produced by PET agents present in tissue. Cherenkov photons are generated when charged particles (such as the positrons emitted by PET imaging agents) travel at a velocity faster than the speed of light in the medium. These emitted Cherenkov photons can be detected with a range of low-cost cameras or small detector technologies. The technique is attractive for
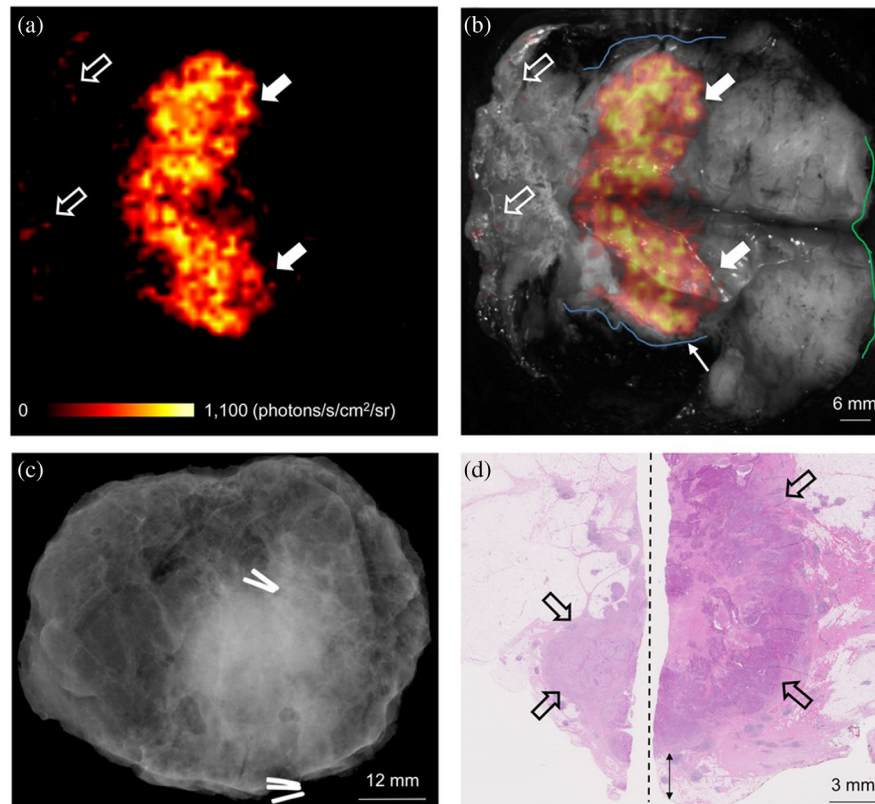
Fig. 4 (a) Cherenkov image of a specimen. White arrows correspond to areas of increased signal where tumor is visible. (b) Photograph of the specimen combined with the Cherenkov signal. (c) Radiography image of the same specimen. (d) H&E image that corresponds to the region.[70] The use of Cherenkov matches the need to obtain surface scan data and provides high resolution, while the key limitations appear to be signal-to-noise possible and the length of the scan time needed. But this modality is in its early stages and further clinical studies will likely occur as the technology evolves. This research was originally published in JNM. Adapted from Ref. 70. Copyright SNMMI.

guiding surgical margins, especially if PET imaging is planned and the imaging agents are already present in the patient.[69] This approach has been used in a study with 18F-fluorodeoxyglucose (FDG) in human patients for intraoperative breast tumor margin assessment. Promising results were found in that elevated tumor radiance was observed at 2.4 times the background tissue, at a dose of only 10's of microSv to surgical staff. However, the study was preliminary (10 patients to optimize the imaging technique followed by 12 that generated the study results), and determining the effectiveness of the technique at margin detection requires further investigation. All 12 margins were negative based on both CLI and standard histology; hence, no results on positive margins were reported. Figure 4 shows a representative case. The Cherenkov signal combined with a greyscale image is compared to radiography and H&E images. Margin status was not estimated accurately from the radiography image due to the presence of a clip.[70] The research is continuing and is being sponsored by LightPoint Medical, Ltd. This technology shows promise especially since it inherently has all of the benefits of standard PET imaging with only minimal additional work. It is a technology for this purpose, so larger studies are needed to show sensitivity and specificity; it can be assumed that they will be at least as good as standard PET imaging however. The drawbacks for CLI imaging are the same as those for standard PET imaging.

3.7 Electromagnetic Measurements

Electromagnetic measurement exploits portions of the electromagnetic spectrum to obtain information about how charge flows through tissue.[71–74] Since biological behavior alters the electromagnetic properties of tissue, these types of measurement methods show promise in detecting changes associated with malignant tumors.

3.7.1 Radiofrequency

Tissues with different structural and molecular characteristics have different electromagnetic scattering, reflectance, and absorbance properties. Radiofrequency spectroscopy considers signals in the radiofrequency range, often delivered by a probe, to determine if the sampled tissue is malignant or benign. One system, "MarginProbe" (Dune Medical Devices, Caesarea, Israel), acquires multiple point measurements from each surface of a specimen and yields a positive or negative reading for each location. If the device outputs a positive result for a given surface, the surgeon removes more tissue from the cavity corresponding to the margin. Measurements of a fully excised lumpectomy require ~5 min. The accuracy of the probe has been compared to standard histology on a set of 753 measurements obtained from 76 breast specimens and was found to have a sensitivity of 70% and a specificity of 70% for all types of

breast malignancies including DCIS. The approach performed better on larger regions of cancers near the surface.[75] A number of clinical trials have been completed with the "MarginProbe" device including the MAST study in Israel, the US Pivotal Study in the United States, and a multicenter study in Germany.[76–78] These studies have led to FDA approval of "MarginProbe" as a device to help surgeons identify positive margins. A more recent study of 596 patients where half the surgeries used the MarginProbe device and half were completed without additional guidance revealed a significant decrease in the number of re-excisions necessary.[79] Radiofrequency imaging offers the potential benefit of an easy to use FDA approved tool for lowering positive margins. However, it also has serious drawbacks of low sensitivity and specificity and it is based on user-guided spot scanning.

3.7.2 Bioimpedance spectroscopy

Another technology that guides surgeons to remove the entire tumor mass is the "ClearEdge"™ (CE) device. It performs bio-impedance spectroscopy on the resected tissue. Bioimpedance spectroscopy is sensitive to intra and extracellular changes in tissue based on alterations in dialectic properties. The CE device is handheld, portable, and battery powered making it very easy to use in the OR. It performs a baseline measurement from the patient's normal breast in order to evaluate differences in cellularity relative to this norm as an internal control. A study involving the CE device reported a re-excision rate of 17% with the system compared to 37% without it as part of the trial. CE completes a full scan in <5 min, the output of which is either green for fatty normal, yellow for fibrous normal, or red for tumor/abnormality, which guides the surgeon to remove more tissue, if needed. This method produced a sensitivity of between 84.3% and 87.3% and a specificity of 75.6% and 81.9%.[80] Bioimpedance spectroscopy is a promising tool due to its fast scanning, portability, and ease of use. However, it lacks sensitivity and specificity and still has a rather large rate of reoccurrence with use.

3.8 Whole Specimen Optical Imaging

Optical methods capture photons to create images. Since photons at optical wavelengths have shallow penetration into tissue, they interrogate the surfaces of tissues effectively for margin analysis, but are limited when assessing internal structures. Whole specimen optical imaging requires wide-field methods and usually scans large areas of tissue to achieve multiple centimeters of coverage. These types of imaging systems tend to have lower spatial resolution than spot sampling, but they also tend to be much faster and cover larger areas of tissue per acquisition.

Current standard of care in BCS involves inking a specimen after removal to maintain specimen orientation during processing.[81] This inking process involves marking each side of the specimen with a specific color of ink so that if a positive margin in found histologically the surgeon will know which side of the cavity to removed tissue from in the re-excision surgery. The timing of this inking is widely variable from institution to institution. Some hospitals now have the surgeon ink immediately after resecting the tissue to preserve orientation while at some the surgeon will place sutures on the specimen which would later be inked in the pathology department. Inking later by the pathologist has been found to be far less accurate

as it is much more difficult to maintain orientation for that period of time.[82,83] One issue that can arise from this inking process is that these colored inks are highly scattering and absorbing with optical and NIR light, which can cause many of the techniques described here to be far less effective. One solution is to use different dyes, which affect NIR light less.[84] Another possibly easier solution would be carefully increasing the "window period" between removal of specimen and inking so that optical techniques can be utilized. During this increased window, the amount of time between resection and inking is not as important as very careful handling to maintain orientation to perform inking after imaging. This is an area of research that must be carefully examined when creating protocols for techniques when they are utilized in clinical settings to not interfere with care.

3.8.1 Photoacoustic tomography

Photoacoustic tomography (PAT) harnesses laser pulses to deliver focal energy to tissue, the absorption of which releases ultrasound emissions. This method achieves contrast through hemoglobin or an exogenous agent and has imaged different types of biological tissues at reasonable depth and with high-chemical selectivity. However, it has not been used extensively for tumor margin detection, since blood-based contrast has not been found to distinguish tumor from other tissue at the margin.[85] One group added a lipid channel as a second contrast, since a large fraction of normal breast contains fat, and acquired data at 16 wavelengths spanning 1100 to 1250 nm. The instrument scanned 4.5 cm^2 of tissue per minute at a 3-mm depth and achieved 125-μm axial resolution, which is sufficient for margin detection. The device achieved 100% sensitivity in a 12-specimen sample set. However, it obtained 75% specificity since dense connective tissue was evaluated to be tumor. Figure 5 shows an example of photoacoustic images and illustrates how the contrast of fat to hemoglobin was used to assess tumor at the margin.[86] Although this method shows promise, large improvement in use and specificity would need to be
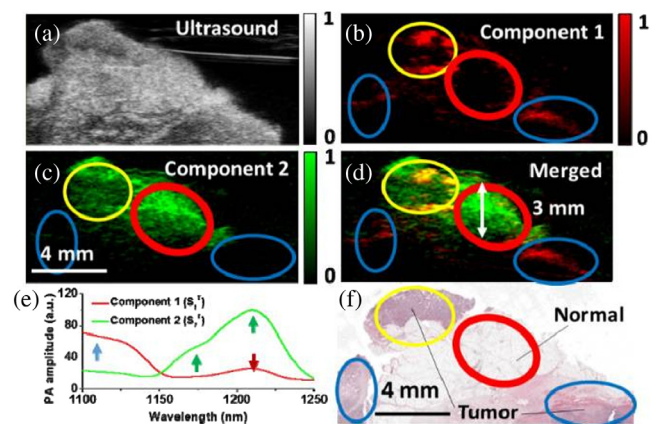
Fig. 5 Example of photoacoustic images of a breast specimen: (a) ultrasound image of the specimen, (b) component 1 shows hemoglobin contrast, (c) component 2 shows adipose contrast, (d) combined Component 1 and component 2 image, (e) spectra of these components, and (f) H&E image corresponding to the regions of interest.[86] This type of imaging shows some potential for deep tissue information albeit at lower spatial resolution than microCT or MRI and tends to have most *ex vivo* contrast based upon fat and water concentrations. Specificity for cellular or molecular features is uncertain at this time. Adapted with permission from Ref. 86, OSA Publishing.

made in order for this technology to be a viable option. The studies to date have been were done on very small sample sizes and comparisons between cancer and healthy tissue only worked well for adipose tissue, not fibroglandular nor connective tissues.

3.8.2 Spatial frequency domain imaging

SFDI, also known as structured light imaging, projects patterns of light at different spatial frequencies and wavelengths to assess the surface of a surgical specimen. Information that can be obtained includes absorption coefficient, reduced scatter coefficient, oxygenated hemoglobin concentration, and deoxygenated hemoglobin concentration.[87] These quantities are biologically relevant to cancer progression. SFDI is also a wide-field process that acquires information over a large surface area quickly. One study applied SFDI to quantify optical properties in the NIR range from 47 lumpectomy specimens. Results distinguished benign from malignant samples with 93% specificity and 79% sensitivity, and all pathology subtypes that were investigated (fibrocystic disease, fibroadenoma, DCIS, invasive cancer, and invasive cancer that was treated with neoadjuvant chemotherapy) were stratified correctly. Figure 6 shows a representative sample of spectral maps created for different tissue categories. For each pathology of tissue present, this figure shows the different optical parameters calculated and the images of these parameters. These maps are used to potentially diagnosis tissue samples.[88] The SFDI process is very fast relative to other methods, provides wide-field and quantitative images, and is very cost-effective compared to other methods. However, it does not provide high-resolution chemical or molecular information.

3.8.3 Fluorescence imaging

Fluorescence imaging records light emitted by a molecule that has absorbed energy from another source. Relative to imaging breast cancer margins, it usually involves injection of a fluorophore preoperatively followed by imaging during surgery or on the resected specimen. One study considered near-infrared (NIR) fluorescence imaging with methylene blue based on the fact that methylene blue should be taken up more in malignant cells and washed out faster in benign tissue. This approach identified tumors in 20 of 24 (83%) of patients. It was better for certain types of breast cancers (carcinomas and DCIS) relative to other subtypes (mucinous). These results are promising but are based on a small number of cases. Figure 7 shows a representative example, in which no fluorescence was detected on the surface of the resected specimen or along the walls of the surgical cavity, but was detected once the specimen was cut and the
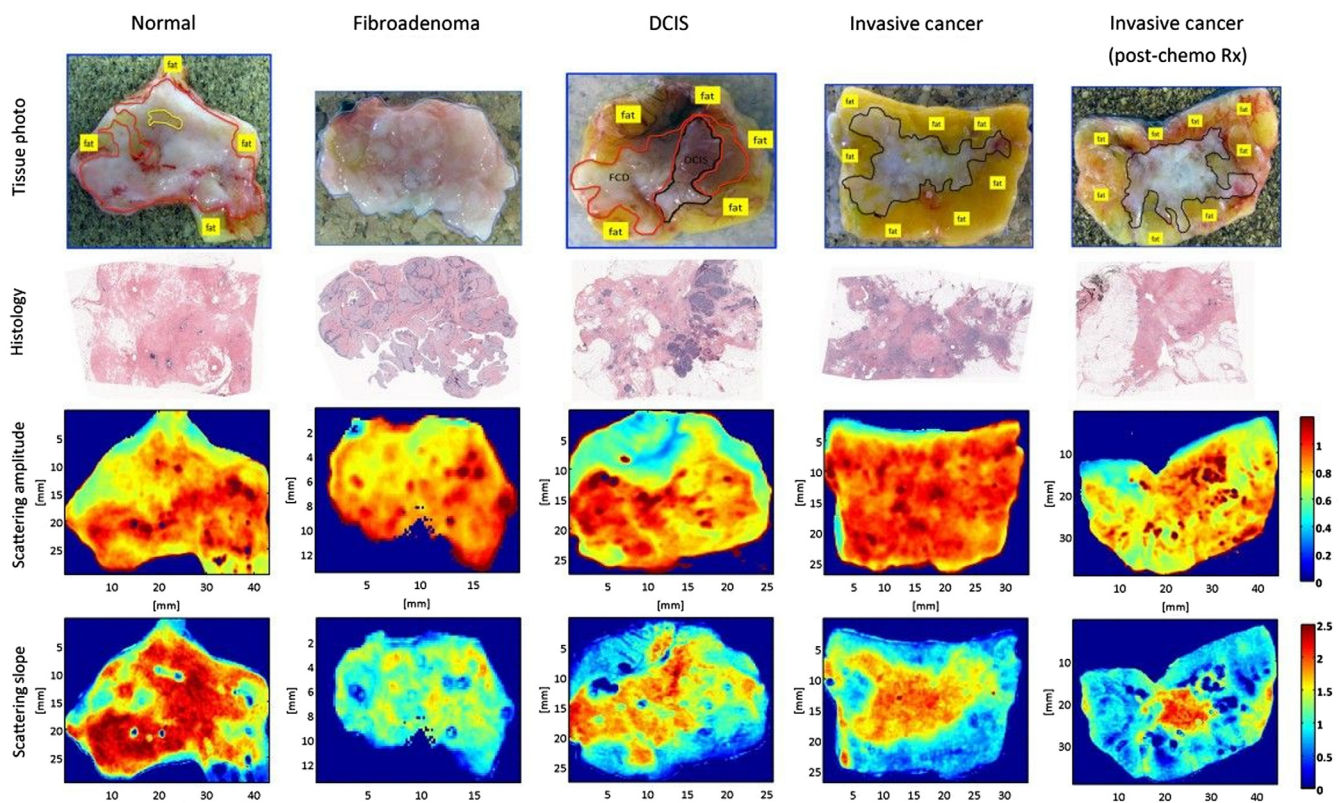
Fig. 6 Spectral maps of different tissue types including normal tissue, fibroadenoma, DCIS, invasive cancer, and invasive cancer postneoadjuvant chemotherapy. Rows include a photograph of the cut specimen (first row) followed by the corresponding H&E images (second row). Spectral maps of scattering amplitude and scattering slope are shown in the latter two rows.[88] This modality provides wide-field full-frame imaging capability with multispectral potential to resolve water, lipids, scattering, and hemoglobin features, at high spatial resolution. The value of this is the high resolution with full optical spectral sensitivity, while the limitations are the fact that this samples largely the surface of the tissue, and so is not volumetric. Adapted from Ref. 88. Creative Commons Attribution License 2.0, Copyright BioMed Central Ltd. .
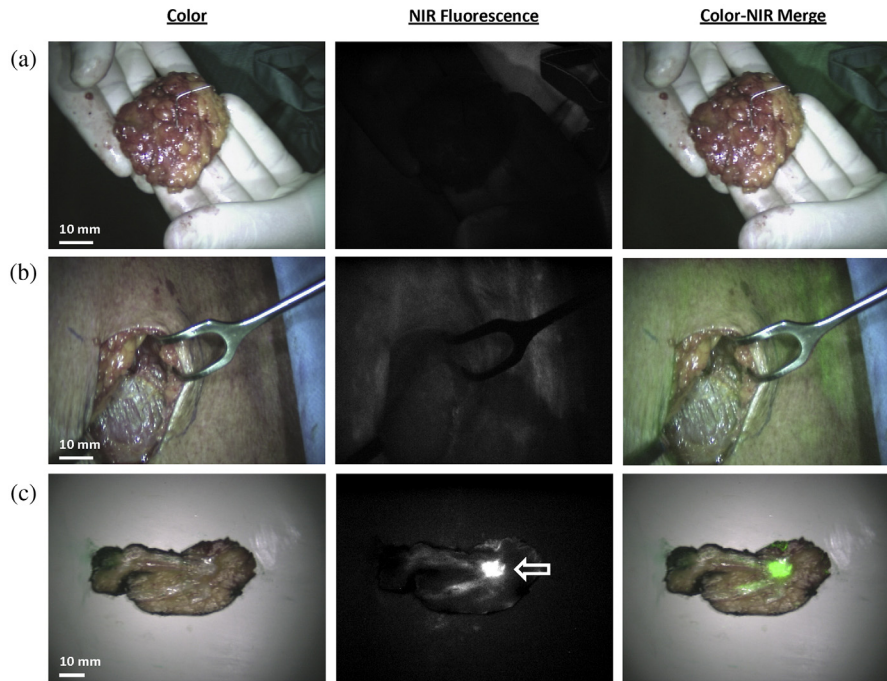
Fig. 7 (a) Resected specimen shows no fluorescent signal, (b) corresponding surgical cavity in which no fluorescent signal was observed, and (c) sliced specimen which shows fluorescent signal at the tumor location.[89] This approach adds significant value by providing a direct surgical view of the tissue and field, but requires contrast injection either prior to or during surgery. The exact contrast available is dependent upon the background tissue and the vascular patency of the tumor and normal tissues. Reprinted with permission from Ref. 89, Copyright 2014, Elsevier.

tumor was revealed.[89] Another NIR fluorophore that is commonly used for sentinel lymph node tracing is indocyanine green.[90] Fluorescence margin assessment has been tested using bevacizumab-IRDye800CW targeting VEGF-A, LUM015, and ABV-620 with some success.[91–93] There are also a number of label-free fluorescence imaging techniques that may show promise for use in BCS. One example of this is using autofluorescense, which uses the body's natural emission sources. In a study of autofluorescense along with diffuse reflectance, one study of 12 patients with tumor surfaces and 28 patients with clinically normal surfaces found an 85% sensitivity and 96% specificity.[94] Another form of label-free fluorescence is fluorescence lifetime imaging (FLIM). This method takes measurements over time after excitation and can separate different fluorophores based on their lifetime. One study using FLIM of resected tissue from 14 patients was able to achieve sensitivities and specificities in the high 90%.[95] Fluorescence imaging shows promise as a method for positive-margin reduction due to its ability to potentially selectively target tumor cells and its ability for real-time imaging. However, it is one of the more invasive methods described here since it involves injecting a fluorophore into the patient and many fluorophores are not selectively targeting in breast tissue.

3.9 Spot Sampling and Microscopic Optical Imaging

Area-sampling optical imaging is similar to whole specimen imaging, except that these methods achieve higher spatial resolution, on the order of cellular features. However, they are usually much slower and are based on scanning techniques, in which many images are acquired and stitched together.

3.9.1 Elastic scatter spectroscopy/diffuse reflectance spectroscopy

Elastic scatter spectroscopy (or diffuse reflectance spectroscopy) applies pulsed or continuous wave light and collects scattered light from the tissue to generate an optical spectrum. One study collected data from 24 patients involving 72 biopsies to classify samples as normal or cancerous. The approach achieved a sensitivity of 67% to 69% and a specificity of 79% to 85%. However, the method of margin detection was based on point measurements and was limited by interference from blood and/or room lights in this preliminary study.[96] This limitation of interference with room lights was because of the preliminary nature of this study and has been solved in later studies.[97]

Both diffuse reflectance spectroscopy and autofluorescence were captured to assess margin status in a data set consisting of 145 normal spectra from 28 patients and 34 tumor spectra from 12 patients. Results yielded a specificity of 96% and a sensitivity of 85% for cancer relative to normal tissue. This method produced a depth sensitivity of about 1 mm for both IDC and DCIS. This is adequate for invasive cancers according to consensus guidelines but for DCIS a margin of 2 mm is recommended. However, changing the geometries of these systems could be a way to obtain a greater depth sensitivity.[94]

Another device was constructed to acquire optical spectral images of tissue using a box that probed a 1×3 cm area. This device used multiple fibers to scan over the specimen in order to create an image. From these images, maps of reduced scatter coefficients and light absorption (total beta-carotene and hemoglobin) were generated. Ratios of total hemoglobin or beta-carotene to the reduced scattering were formed in an average of 25 s per image area. These two ratios were evaluated to

distinguish positive or close margins from a clear margin. The study yielded a sensitivity of 79.4% and a specificity of 66.7% on an imaging set of 48 patients and showed that the ratio of beta-carotene to reduced scatter was a better indicator of margin status than the hemoglobin to reduced scatter ratio.[98] Another study used diffuse reflectance spectroscopy with two different models to compare the diagnostic value of each. When using a Monte Carlo-based model, they were able to achieve a sensitivity of 83% and a specificity of 80%. They also used an empirical partial least squares model and were able to achieve a sensitivity of 83% and a specificity of 76%.[99]

Another study used light with wavelengths between 500 and 1600 nm for diffuse optical spectroscopy on a set of 102 samples. From these optical measurements, several parameters such as blood, water, and lipid volume fractions, Mie slope, Mie scatter fraction, reduced scattering amplitude, and pigment packaging factor were computed and analyzed for their diagnostic power. This study found high sensitivity (between 81% and 98% depending on the tissue type) and high selectivity (95% to 99%). This study also noted that commonly beta-carotene is used as an adipose discriminator but that lipid volume fraction was found to be a better discriminator in this study.[100] Diffuse reflectance spectroscopy offers potentially high specificity and selectivity and is able to give a significant amount of useful information about the tissue. However, it is probe based, which leads to a good potential for user error and can take a significant amount of time to get an adequate amount of tissue sampled.

3.9.2 MUSE

Microscopy with UV surface excitation (MUSE) exploits the low-penetration depth of UV light to excite fluorophores at the surface of a stained tissue. The approach is relevant to margin assessment of invasive tissue in BCS, since guidelines suggest that "tumor on ink"[4] is the requirement for a positive margin in the case of invasive cancers. It is rapid, inexpensive, and nondamaging to tissue samples and does not require the steps associated with conventional histology processing, fixing, embedding, or sectioning. MUSE does use a fluorescence dye to stain tissue. It is not useful if depth information is necessary (e.g., when assessing a positive margin for DCIS) since it relies on the shallow penetration depth of UV light, and as a result interrogates the surface of the resected specimen.[101,102] Since MUSE is still in its infancy as a technique for breast tumor margin assessment, large scale studies are required to get sensitivity and specificity numbers. MUSE offers excellent information for invasive cancer margin detection but needs further study before it can be seen as a solution to the positive margin problem.

3.9.3 Light-sheet microscopy

Light-sheet microscopy uses decoupled illumination and collection beams for fluorescence generation and detection in order to achieve both rapid imaging of irregular surfaces and depth imaging of volumetric samples. A recent study reported the ability to image a 4-cm^2 tissue surface stained in acridine orange in less than a minute with an open-top light-sheet microscopy system and obtained similar information to conventional H&E staining and imaging. Figure 8 shows a representative comparison of light-sheet microscopy with H&E imaging. This shows how light-sheet microscopy matches very well with histology and better than frozen section analysis.[103] Light-sheet microscopy is a technology that has not been applied to a large enough study yet to obtain sensitivity and specificity measurements. Light-sheet microscopy provides excellent resolution and information about the tissue surface. However, it does this at the expensive of potentially long scan times and providing too much information to digest in a surgical environment.
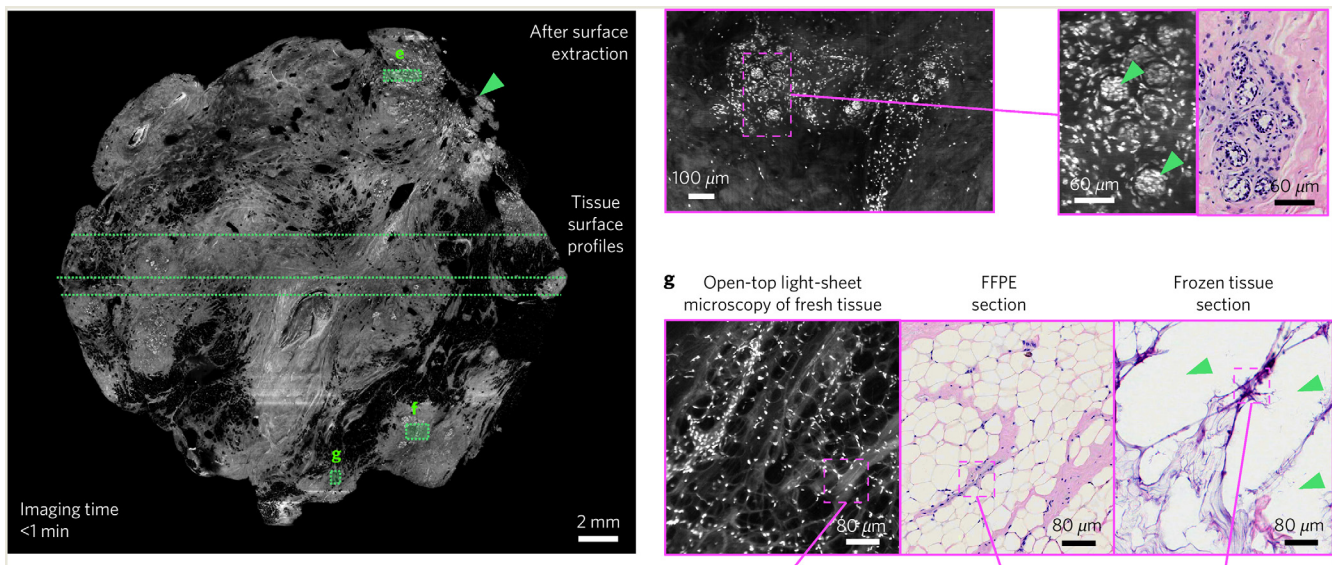
Fig. 8 Images comparing the performance of light-sheet microscopy with histology. Images of different regions with different magnifications and their corresponding histology images are shown. Results from frozen-sectioning imaging are also included and suggest improved performance with light-sheet microscopy.[103] The value of this type of system is the extremely high spatial resolution and the ability to augment pathology imaging, whereas the limitations here are the fact that the scan times could be lengthy and the information could be too dense for surgical use. Reprinted by permission from Ref. 103, Springer Nature.
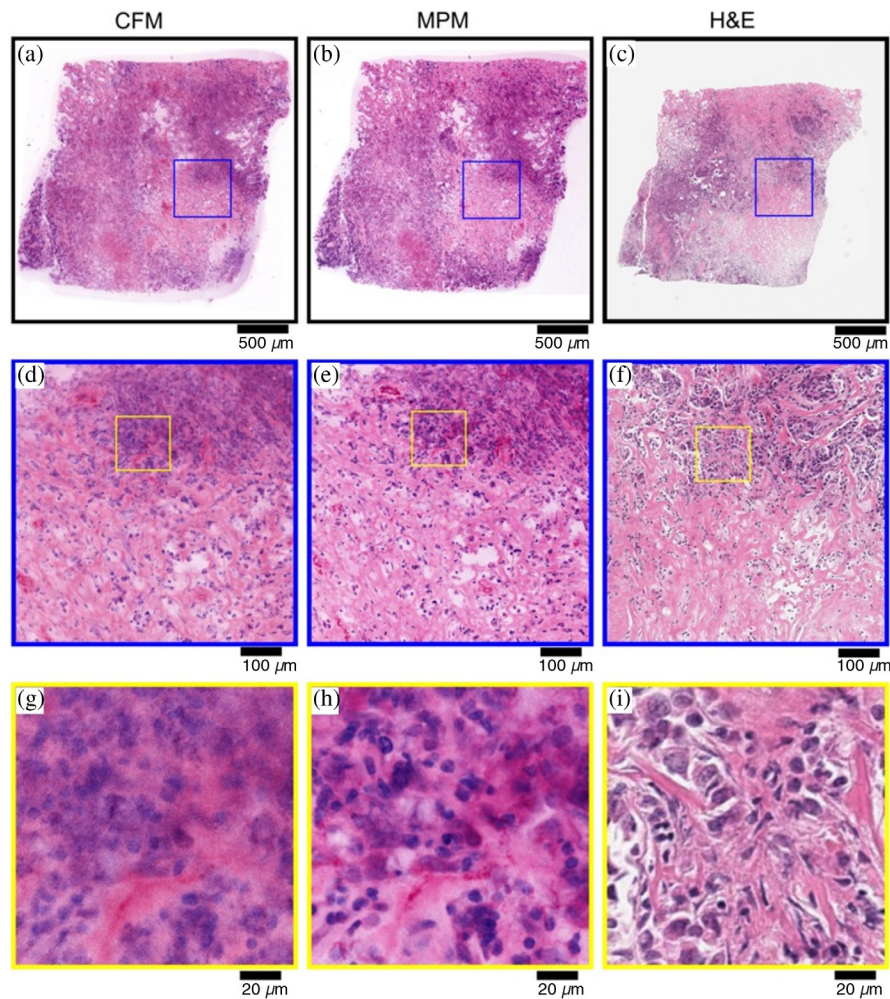
Fig. 9 Images of the same specimen with invasive ductal carcinoma obtained with CFM, multiphoton microscopy (MPM), and H&E histology. The left column shows images from CFM, the middle column is MPM, and the right column is the H&E results. Each row shows a corresponding magnification of the image data.[106] These scans are at the pathology imaging level and so while extremely rich in information, they provide a better solution for pathologists than for surgical guidance. Adapted with permission from Ref. 106, SPIE Publishing.

3.9.4 Nonlinear microscopy

Several types of nonlinear microscopies are available and include incoherent nonlinear methods such as two-photon fluorescence as well as coherent nonlinear approaches such as second harmonic signal generation or coherent anti-Stokes Raman scattering.[104]

One study evaluated 179 specimens from 50 patients to determine if nonlinear microscopy has merit for intraoperative margin assessment. Two-photon microscopy was acquired from samples that were stained with acridine orange for nuclear imaging. The approach offered the benefit that data were obtained on fresh intact samples without a need for sectioning, fixing, or embedding associated with other methods such as frozen sectioning, although extrinsic staining with acridine orange was required. Resulting images were false-colored to match closely the colors that would appear with H&E staining in order to present familiar information to the pathologist. This false coloring used to create these pseudo-H&E slides came from the two-photon fluorescence from acridine orange for the blue and the second harmonic generation for the pink areas representing

collagen. Results showed 95.4% sensitivity and 93.3% specificity on average in classifying benign and invasive cancer samples relative to corresponding H&E diagnoses.[105] Figure 9 shows nonlinear microscopy images acquired from a specimen with invasive ductal carcinoma and compares them to confocal fluorescence and H&E images. This shows the correlation between the false-color images created using nonlinear microscopy and H&E images.[106] The study concluded that confocal florescence microscopy offered similar information to nonlinear microscopy, but at much lower cost. When magnification was increased significantly, a blurring effect did occur with confocal fluorescence microscopy (CFM); however, nonlinear microscopy offers molecular information with very strong sensitivity and specificity. However, its largest drawbacks are its small region sampling leading to long scan times if large area coverage is wanted and its cost due to the high cost of the short-pulse lasers used.

3.9.5 Optical coherence tomography

Optical coherence tomography (OCT) applies NIR light to create micron-scale images of subsurface tissue structure up to

2 mm below the surface. Data can be produced in real time and are multidimensional. OCT takes advantage of the highly scattering nature of tumor cells (because of their higher nucleus-to-cytoplasm ratio) relative to the large, low-scattering behavior of adipose cells. When used to determine margin status, OCT identifies regions of highly scattering, heterogeneously scattering, and tightly packed cells. Cauterized tissue and surface blood can interfere with OCT; however, these effects are visually apparent on the sample before OCT acquisition. The highly scattering characteristic of cancerous cells and their heterogeneity can also be distinguished from the low scattering of blood and cauterized tissue which are largely confined to the surface of the sample. In a study of 20 patients, OCT yielded a specificity of 82% and a sensitivity of 100% (9 true positives, 9 true negatives, 2 false positives, and 0 false negatives) in predicting margin status of lumpectomy specimens. Dyes do not affect OCT since they absorb in the lower wavelengths of light; for example, around 1300 nm in this study. Scans of 1 cm^2 surface regions of tissue can be acquired in seconds with a lateral resolution of 35 μm. However, it is worth noting that lumpectomy sites are usually larger than 1 cm^2, so this could take several minutes to analyze based on how large the sample is and the amount of time it would take to rotate the sample. OCT can be used both in the resected specimen and in the surgical cavity. A representative sample, which includes normal tissue, common artifacts such as those caused by blood or cauterized tissue, and tumor is shown in Fig. 10.[107] A handheld probe was swept across a tumor bed or a resected sample similarly to the way conventional ultrasound is used. Here, data from 35 patients yielded an average sensitivity of 91.7% and an average specificity of 92.1% based on image assessments provided by five trained OCT readers.[108] Another study evaluated specimens from 46 patients at 2 different hospitals with a handheld OCT probe, which also invoked interferometric synthetic aperture image processing read by three trained physicians. This study acquired 2191 images of 229 shaved margins obtained from these patients. The device achieved a sensitivity of 55% to 65% and a specificity of 68% to 70%.[109] OCT images require a trained reader who must be in the OR at time of surgery, which is labor-intensive and logistically difficult. There are also companies such as Perimeter Medical which are developing commercial systems for intraoperative OCT.[110] OCT offers high resolution, depth scans in real time, which makes it an attractive technology for use in lowering the number of positive margins. However, 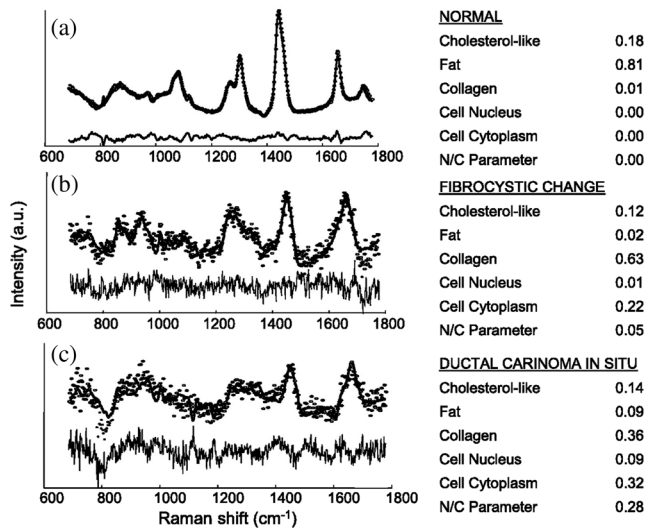it has some serious drawbacks including the need for a trained operator to be present of the surgery and that it is spot sampling so it requires potentially long times to scan the entire specimen.

3.9.6 Raman spectroscopy

Raman spectroscopy sources monochromatic light in the visible, NIR, or near-ultraviolet range to obtain chemical information about a sample. It exploits the Raman effect or inelastic scattering of photons to virtual energy states, and their resulting gain or loss of energy from interactions with vibrational modes of the material being interrogated. The effect is measured through shifts in energy caused by the phenomenon. Certain shifts are known to be associated with specific types of biological material, which indicates Raman spectroscopy can be very sensitive to the biochemical makeup of tissue. Raman spectroscopy is very specific to the molecular makeup on the region analyzed; however, signal intensity is weak. Since these signal levels are low, data acquisition may need to involve long collection times, which are nonideal for a surgical setting. Raman spectroscopy produces information at a subcellular level noninvasively, label-free and is not contaminated by water. It detected margin status with 93.3% accuracy on a data set of 31 spectra acquired from 9 patients. Unfortunately, the data set contained only one positive margin and is limited in this regard. The method also depends on point measurements and records spectra at a rate of 1 Hz. Figure 11 shows Raman spectra from this study for normal breast tissue, fibrocystic change, and DCIS, along with their corresponding coefficients.[111] Another study developed a probe that used spatial-offset raman spectroscopy to determine margin status up to 2 mm below the surface of excised specimens with 95% sensitivity and 100% specificity in 35 samples. However, the system acquired point measurements which caused the margin assessments to be laborious and time-intensive.[112] Another study reported results from a device, "Marginbot," which is an automated scanning system for the surface of a tissue sample. The instrument automatically scanned the surface of the sample using a probe-based system and provided its margin status in <15 min. It distinguished fibroadenoma from fatty areas of mastectomy samples with 93% sensitivity and 85% specificity, but these positive results are yet to be replicated in true lumpectomy specimens since this study used mastectomy samples.[113] Raman spectroscopy offers chemical information about the tissue noninvasively, which is a benefit for identifying positive margins in BCS. However, the technology has large drawbacks
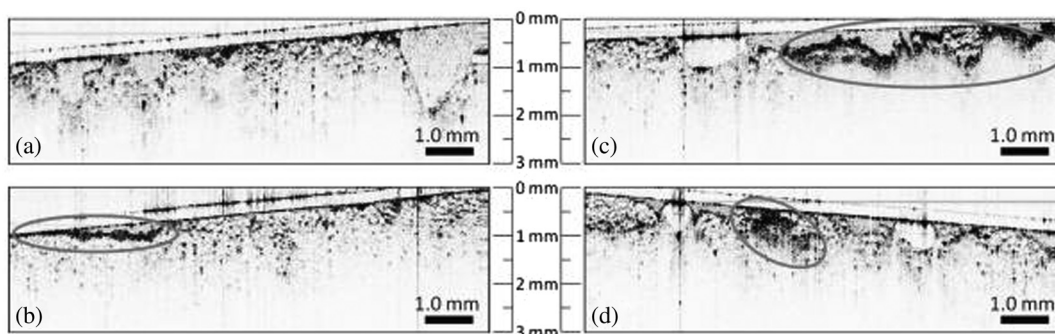
Fig. 10 Representative OCT images of margins from resected tissue samples including: (a) normal tissue, (b) artifacts such as blood, (c) cauterized tissue, and (d) tumor cells at the margin.[107] Adapted with permission from Ref. 107, AACR.

NORMAL	
Cholesterol-like	0.18
Fat	0.81
Collagen	0.01
Cell Nucleus	0.00
Cell Cytoplasm	0.00
N/C Parameter	0.00

FIBROCYSTIC CHANGE	
Cholesterol-like	0.12
Fat	0.02
Collagen	0.63
Cell Nucleus	0.01
Cell Cytoplasm	0.22
N/C Parameter	0.05

DUCTAL CARINOMA IN SITU	
Cholesterol-like	0.14
Fat	0.09
Collagen	0.36
Cell Nucleus	0.09
Cell Cytoplasm	0.32
N/C Parameter	0.28

Fig. 11 Raman spectra and fit coefficients for (a) normal breast tissue, (b) fibrocystic change, and (c) DCIS.[111] The use of Raman has progressed to mapping, but the low-signal levels have limited to point sampling largely from imaging, and so the major barrier in this area has been the logistics of application in a time efficient manner to large specimens. But the attraction to having native molecular specific information about the tissue has always been a driving factor in utilizing this methodology for true molecular specific detection of disease. Adapted with permission from Ref. 111, AACR.

for BCS including that it is spot-sampling-based and that it requires long scan times that would likely be too long for use in a surgical setting.

Another form of Raman scattering is found in Raman-encoded molecular imaging (REMI), which incorporates nanoparticles that are surface-enhanced Raman-scattering (SERS) entities that are topically applied to specimen surfaces. One study evaluated both targeted and nontargeted SERS nanoparticles and their concentration ratios to determine the presence of malignancy at the tissue surface. Four biomarkers, HER2, mER, EGFR, and CD44, were considered. Tissue was stained, rinsed, and raster scanned to create an image that was spectrally demultiplexed in about 10 to 15 min. Sensitivity of 89.3% and specificity of 92.1% were found based on over-expression of one or more of these biomarkers. This imaging method is only applicable to the tissue surface, thus, it is not able to tell if margins are clear 2 mm below the surface for DCIS.[114] REMI is attractive as a technology for use in identifying positive margins since it gives relevant biological information in these biomarkers. It does suffer from the need for use of applied nanoparticles and long scan times.

4 Discussion

Table 2 lists each of the techniques discussed in this review and how they compare based on common clinical and technical concerns. Each technique offers benefits and pitfalls. These rankings are based upon each modality's strengths and weaknesses as discussed based on the literature cited earlier. The scores and weights reflect a consensus statement by the authors of this paper. Some of the criteria are more subjective than others. The best approaches according to Table 2 criteria appear to be SFDI, bioimpedance spectroscopy, and radiofrequency. The best method for imaging the interior of specimens to discern

tumor extent is micro-CT. Overall, optical methods show the most promise because they collect information quickly and some achieve the penetration depths required to meet current consensus definitions of clear margins.

It may be important to note that although the focus of this review is on techniques which take measurements of resected tissue, it is possible to use some of these techniques directly on the cavity wall *in vivo*. This comes with both benefits and pitfalls. The largest benefit would be that if imaging the tumor bed, the surgeon can immediately remove the exact area where the malignancy is rather than basis the resecting on where on the removed tissue contains a positive margin. A rather large drawback of this is that the conditions for measuring are far less able to be controlled such as background lighting and blood. Cavity walls are unable to be registered with pathology as well, unless extra tissue is removed after measurement.

4.1 Hybrid Systems

Systems that incorporate multiple types of complementary imaging to yield a more complete picture of the resected tissue may offer more complete advantages. An example might be a radiographic system used to obtain 3-D image data on internal structure and tumor confirmation inside the resected specimen tissue, combined with an optical system to gain more detailed image data on surface margins. Radiological systems tend not to be very accurate in assessing tumor at specimen surfaces while optical systems often have limited penetration depth and provide less information about the interior of the tissue. Another hybrid approach might be one where a system provides interior imaging that guides application of a second, specific, high-accuracy approach, which involves more time and effort to use. For example, combining a wide-field imaging approach with a point assessment system to yield new information is an appealing strategy. According to Table 2, the best system for assessing the specimen interior and tissue volume is micro-CT, whereas the best systems for evaluating the tissue surface are SFDI, spectral imaging, and radiofrequency imaging. Figure 12 shows an example of a hybrid system that combines SFDI with a micro-CT scanner. This pair may be ideal because each subsystem provides complementary information. Micro-CT provides tumor confirmation and localization and guides localization of the SFDI acquisition, which offers much better information on margin status at the surface of the specimen.

5 Conclusions

Significant clinical need exists for better margin detection intraoperatively because 15% to 35% of BCS patients need a second surgery to remove more tissue when a positive margin is found. Several methods are available that are already part of standard-of-care but they all have significant clinical and technical limitations that have precluded wide-spread adoption. A number of methods are being investigated to meet the clinical need better. This paper reviewed a number of these approaches and compares them in terms of clinical and technical criteria. Based on these comparisons, the most promising techniques for margin detection are optical methods based on their rapid acquisition of image data, nondestructive characteristics, and penetration depths sufficient to meet consensus guidelines for establishing clear margins in BCS.

Technologies to determine margin status have been developed to have high sensitivity and selectivity. However, no current modality has matured into a complete solution to the margin

Table 2 Techniques discussed in this review weighted by common clinical and logistical concerns. Scores of 1 are the lower and scores of 5 are the best. The clinical issue sections such as tumor extent inside, surface for invasive, and 2 mm for DCIS scores are based upon the modality's ability to measure at that scale and the resolution of the system at that scale. The lack of user/reader necessity ranking is based on the amount of extra staff and training needed to use the modality. Interior versus surface shows whether a system measures through the whole specimen or if it measures the surface to look for malignancy. For the section short time, a relative ranking was given rather than exact measurement times due to the evolving nature of many of these modalities. Times are for preparation and measurement time. These relative times are grouped as follows: a score of 1 is days, a score of 2 is roughly an hour, a score of 3 is in the tens of minutes, and a score of 4 is in minutes. Robust performance involves the ruggedness of the measurements as well as the amount of data reproducibility.

Issues/desirs	Weight	Radio-graphic	Micro-CT	MRI	PET/CT	CLI	Radio frequency	HF ultra-sound	Bioimpedance spectroscopy	PAT	SFDI	DRS	ESS/Fluores-cence	MUSE	Light-sheet microscopy	Nonlinear microscopy	OCT	Raman	Frozen sectioning	Imprint cytology	Permanent hist
Clinical																					
Large area scan	4	5	5	4	4	3	1	2	2	4	5	2	5	4	4	1	2	1	1	4	4
Extent of tumor inside/tumor confirmation	5	4	5	4	5	2	1	2	1	2	2	1	1	1	1	1	2	3	1	1	5
Surface for invasive	5	1	2	1	1	4	4	1	3	3	4	3	3	5	5	5	4	4	5	4	5
2-mm depth for DCIS	5	1	2	1	1	4	4	4	4	3	4	2	3	3	3	4	3	3	3	3	5
Lack of user/reader necessity	3	2	2	1	3	5	3	3	5	4	4	3	5	4	4	2	2	2	1	1	1
Logistical/technical																					
Interior (I) versus surface (S) view		I	I	I	I/S	S	S	S	S	S	S	S	S	S	S	S	S	S	S	S	I/S
Spot-based (S) versus wide field (W)		W	W	W	W	W	S	S	S	W	W	S	W	W	W	S	S	S	S	S	S
Small data volume	2	2	2	3	4	2	2	2	2	3	2	2	4	1	1	1	4	3	3	4	1
Short time	3	4	3	3	2	3	4	4	4	4	4	4	4	3	3	2	4	2	2	3	1
Lack of processing/stain	3	2	2	2	1	1	5	5	5	4	5	5	1	2	2	2	1	3	1	3	1
Robust performance	4	5	5	5	4	2	4	3	3	2	4	3	4	5	4	1	4	3	4	4	5
Small footprint	3	1	3	1	1	3	5	5	5	4	4	4	3	4	3	2	4	3	2	2	1
Sensitivity	5	1	2	5	5	2	1	4	3	5	5	3	4	1	1	5	3	5	4	3	5
Specificity	4	3	5	2	4	1	2	5	4	3	3	5	2	1	1	5	5	5	5	5	5
Low cost	4	4	3	2	1	2	4	4	5	3	5	5	4	5	3	2	4	2	5	5	4
Total		134	161	134	135	121	164	151	177	161	198	157	162	151	136	137	157	155	149	162	186
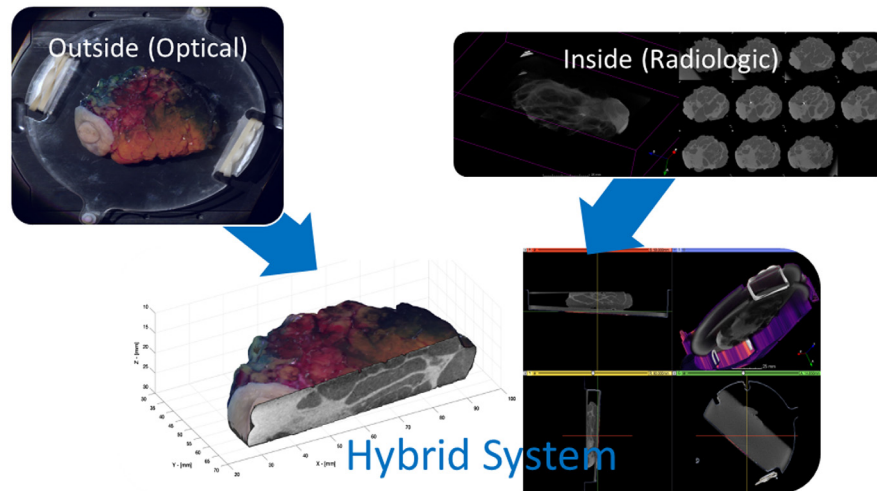
Fig. 12 Example hybrid system which combines an SFDI optical method with micro-CT. The micro-CT provides tumor confirmation from the volumetric scan through the sample and localization information on the margins, while the optical imaging of the surface is sensitive to cancer tumor on the surface of the specimen. The value of this hybrid approach is to solve both needs for highly accurate internal anatomy of the tumor with highly accurate surface scanning for involved margin regions. While this is one example of a possible system, the solutions of volumetric for anatomy and surface for molecular/cellular sensitivity appear to be an important requirement for any viable solution.

problem currently facing BCS. Ideally, a system would be able to detect malignancy on the surface quickly while keeping false positive margins low to avoid removing excess tissue. Ideally, but less importantly, a system would be able to confirm tumor localization as well as determining margin status. This would prove that not only is there not tumor on the surface, but also that the tumor is contained within the resected tissue. The ideal system would also need to be rapid, low-cost, and easy to use, with sensitivity near 95% and specificity near 85%. As technologies evolve, they will have to be tested in appropriate single-center then multicenter trials to confirm their performance metrics.

Disclosures

No conflicts of interest, financial or otherwise, are declared by the authors.

Acknowledgments

References

1. A. I. Mushlin, R. W. Kouides, and D. E. Shapiro, "Estimating the accuracy of screening mammography: a meta-analysis," *Am. J. Prev. Med.* **14**(2), 143–153 (1998).
2. R. L. Siegel, K. D. Miller, and A. Jemal, "Cancer statistics, 2016," *CA Cancer J. Clin.* **66**(1), 7–30 (2016).
3. U. Veronesi et al., "Twenty-year follow-up of a randomized study comparing breast-conserving surgery with radical mastectomy for early breast cancer," *N. Engl. J. Med.* **347**(16), 1227–1232 (2002).
4. M. S. Moran et al., "Society of Surgical Oncology-American Society for Radiation Oncology Consensus Guideline on margins for breast-conserving surgery with whole-breast irradiation in stages I and II invasive breast cancer," *Ann. Surg. Oncol.* **21**(3), 704–716 (2014).
5. M. Morrow et al., "Society of Surgical Oncology-American Society for Radiation Oncology-American Society of Clinical Oncology Consensus Guideline on margins for breast-conserving surgery with whole-breast irradiation in ductal carcinoma in situ," *Pract. Radiat. Oncol.* **6**(5), 287–295 (2016).
6. M. S. Anscher et al., "Local failure and margin status in early-stage breast carcinoma treated with conservation surgery and radiation therapy," *Ann. Surg.* **218**(1), 22–28 (1993).
7. D. H. Roukos, A. M. Kappas, and N. J. Agnantis, "Perspectives and risks of breast-conservation therapy for breast cancer," *Ann. Surg. Oncol.* **10**(7), 718–721 (2003).
8. M. M. Moore et al., "Association of infiltrating lobular carcinoma with positive surgical margins after breast-conservation therapy," *Ann. Surg.* **231**(6), 877–882 (2000).
9. N. Cabioglu et al., "Role for intraoperative margin assessment in patients undergoing breast-conserving surgery," *Ann. Surg. Oncol.* **14**(4), 1458–1471 (2007).
10. R. J. Gray et al., "Intraoperative margin management in breast-conserving surgery: a systematic review of the literature," *Ann. Surg. Oncol.* **25**(1), 18–27 (2018).
11. D. Dumitru, M. Douek, and J. R. Benson, "Novel techniques for intraoperative assessment of margin involvement," *Ecancermedicalscience* **12**, 795 (2018).
12. F. J. Fleming et al., "Intraoperative margin assessment and re-excision rate in breast conserving surgery," *Eur. J. Surg. Oncol.* **30**(3), 233–237 (2004).
13. G. C. Balch et al., "Accuracy of intraoperative gross examination of surgical margin status in women undergoing partial mastectomy for breast malignancy," *Am. Surg.* **71**(1), 22–27; discussion 27–28 (2005).
14. P. J. Lovrics et al., "The relationship between surgical factors and margin status after breast-conservation surgery for early stage breast cancer," *Am. J. Surg.* **197**(6), 740–746 (2009).
15. P. J. Lovrics et al., "Technical factors, surgeon case volume and positive margin rates after breast conservation surgery for early-stage breast cancer," *Can. J. Surg.* **53**(5), 305–312 (2010).
16. H. D. Nelson et al., "Effectiveness of breast cancer screening: systematic review and meta-analysis to update the 2009 U.S. preventive services task force recommendation," *Ann. Intern. Med.* **164**(4), 244–255 (2016).
17. C. S. Lee et al., "Harmonizing breast cancer screening recommendations: metrics and accountability," *Am. J. Roentgenol.* **210**(2), 241–245 (2017).
18. H. G. Welch and H. J. Passow, "Quantifying the benefits and harms of screening mammography," *JAMA Intern. Med.* **174**(3), 448–453 (2014).

19. J. M. Park et al., "Breast tomosynthesis: present considerations and future applications," *Radiographics*, **27**(Suppl 1), S231–S240 (2007).
20. W. A. Berg et al., "Combined screening with ultrasound and mammography vs mammography alone in women at elevated risk of breast cancer," *J. Am. Med. Assoc.* **299**(18), 2151–2163 (2008).
21. W. A. Berg et al., "Detection of breast cancer with addition of annual screening ultrasound or a single screening MRI to mammography in women with elevated breast cancer risk," *J. Am. Med. Assoc.* **307**(13), 1394–1404 (2012).
22. D. Saslow et al., "American Cancer Society guidelines for breast screening with MRI as an adjunct to mammography," *CA Cancer J. Clin.* **57**(2), 75–89 (2007).
23. M. Kriege et al., "Efficacy of MRI and mammography for breast-cancer screening in women with a familial or genetic predisposition," *N. Engl. J. Med.* **351**(5), 427–437 (2004).
24. M. Funke, "Diagnostic imaging of breast cancer: an update," *Radiology* **56**(10), 921–938 (2016).
25. H. Zhi et al., "Comparison of ultrasound elastography, mammography, and sonography in the diagnosis of solid breast lesions," *J. Ultrasound Med.* **26**(6), 807–815 (2007).
26. N. R. Epstein, P. M. Meaney, and K. D. Paulsen, "3D parallel-detection microwave tomography for clinical breast imaging," *Rev. Sci. Instrum.* **85**(12), 124704 (2014).
27. S. G. Orel et al., "Staging of suspected breast cancer: effect of MR imaging and MR-guided biopsy," *Radiology*, **196**(1), 115–122 (1995).
28. M. D. Den Hartogh et al., "MRI and CT imaging for preoperative target volume delineation in breast-conserving therapy," *Radiat. Oncol.* **9**, 63 (2014).
29. F. D. Rahusen et al., "Ultrasound-guided lumpectomy of nonpalpable breast cancer versus wire-guided resection: a randomized clinical trial," *Ann. Surg. Oncol.* **9**(10), 994–998 (2002).
30. P. J. Lovrics et al., "A multicentered, randomized, controlled trial comparing radioguided seed localization to standard wire localization for nonpalpable, invasive and in situ breast carcinomas," *Ann. Surg. Oncol.* **18**(12), 3407–3414 (2011).
31. S. E. Singletary, "Surgical margins in patients with early-stage breast cancer treated with breast conservation therapy," *Am. J. Surg.* **184**(5), 383–393 (2002).
32. R. Laucirica, "Intraoperative assessment of the breast: guidelines and potential pitfalls," *Arch. Pathol. Lab. Med.* **129**(12), 1565–1574 (2005).
33. J. C. Cendan, D. Coco, and E. M. Copeland 3rd, "Accuracy of intraoperative frozen-section analysis of breast cancer lumpectomy-bed margins," *J. Am. Coll. Surg.* **201**(2), 194–198 (2005).
34. J. M. Jorns et al., "Intraoperative frozen section analysis of margins in breast conserving surgery significantly decreases reoperative rates: one-year experience at an ambulatory surgical center," *Am. J. Clin. Pathol.* **138**(5), 657–669 (2012).
35. K. Esbona, Z. Li, and L. G. Wilke, "Intraoperative imprint cytology and frozen section pathology for margin assessment in breast conservation surgery: a systematic review," *Ann. Surg. Oncol.* **19**(10), 3236–3245 (2012).
36. E. Weinberg et al., "Local recurrence in lumpectomy patients after imprint cytology margin evaluation," *Am. J. Surg.* **188**(4), 349–354 (2004).
37. P. Elmer, "IVIS SpectrumCT product note," https://www.perkinelmer.com/lab-solutions/resources/docs/BRO_010459C_01%20PRD_SpectrumCT.pdf (11 January 2018).
38. Bruker, "Skyscan 1173: World's first spiral micro-CT," http://bruker-microct.com/products/1173.html (11 January 2018).
39. Services D.o.H.a.H, "Biovision (plus/+) digital specimen radiography (DSR) system: FDA 510(k) Summary," 2016, https://www.accessdata.fda.gov/cdrh_docs/pdf15/K153583.pdf (11 January 2018).
40. FDA, "Pathvision specimen radiography system: FDA 510(k) summary," 2012, https://www.accessdata.fda.gov/cdrh_docs/pdf12/K122428.pdf (11 January 2018).
41. FDA, "Hologic trident specimen radiography system, model: RC: FDA 510(k) summary," 2011, https://www.fda.gov/cdrh/510k/K111508.pdf (11 January 2018).
42. C. S. Kaufman et al., "Intraoperative digital specimen mammography: rapid, accurate results expedite surgery," *Ann. Surg. Oncol.* **14**(4), 1478–1485 (2007).
43. S. H. Kim et al., "An evaluation of intraoperative digital specimen mammography versus conventional specimen radiography for the excision of nonpalpable breast lesions," *Am. J. Surg.* **205**(6), 703–710 (2013).
44. K. C. Young et al., "Optimal beam quality selection in digital mammography," *Br. J. Radiol.* **79**(948), 981–990 (2006).
45. Faxitron, "Faxitron wedge," 2017, https://www.faxitron.com/product/wedge/ (5 January 2018).
46. A. B. Chagpar et al., "Does three-dimensional intraoperative specimen imaging reduce the need for re-excision in breast cancer patients? A prospective cohort study," *Am. J. Surg.* **210**(5), 886–890 (2015).
47. M. Urano et al., "Digital mammography versus digital breast tomosynthesis for detection of breast cancer in the intraoperative specimen during breast-conserving surgery," *Breast Cancer* **23**(5), 706–711 (2016).
48. R. Tang et al., "Micro-computed tomography (Micro-CT): a novel approach for intraoperative breast cancer specimen imaging," *Breast Cancer Res. Treat.* **139**(2), 311–316 (2013).
49. I. Willekens et al., "High-resolution 3D micro-CT imaging of breast microcalcifications: a preliminary analysis," *BMC Cancer* **14**, 9 (2014).
50. H. Nishide, T. Kasuga, and T. Miyachi, "Report on the 89th scientific assembly and annual meeting of the Radiological Society of North America—micro-focus x-ray CT imaging of breast specimens with microcalcifications," *Nihon Hoshasen Gijutsu Gakkai Zasshi* **60**(12), 1662–1663 (2004).
51. D. M. McClatchy et al., "Calibration and analysis of a multimodal micro-CT and structured light imaging system for the evaluation of excised breast tissue," *Phys. Med. Biol.* **62**(23), 8983–9000 (2017).
52. S. Q. Qiu et al., "Micro-computed tomography (micro-CT) for intraoperative surgical margin assessment of breast cancer: a feasibility study in breast conserving surgery," *Eur. J. Surg. Oncol.* (2018).
53. D. M. McClatchy, III et al., "Micro-computed tomography enables rapid surgical margin assessment during breast conserving surgery (BCS): correlation of whole BCS micro-CT readings to final histopathology," *Breast Cancer Res. Treat.* (2018).
54. J. E. Tan et al., "Role of magnetic resonance imaging and magnetic resonance imaging-guided surgery in the evaluation of patients with early-stage breast cancer for breast conservation treatment," *Am. J. Clin. Oncol.* **22**(4), 414–418 (1999).
55. U. Fischer, L. Kopka, and E. Grabbe, "Breast carcinoma: effect of preoperative contrast-enhanced MR imaging on the therapeutic approach," *Radiology* **213**(3), 881–888 (1999).
56. S. G. Orel, "MR imaging of the breast," *Magn. Reson. Imaging Clin. N. Am.* **9**(2), 273–288 (2001).
57. M. V. Hill et al., "Relationship of breast MRI to recurrence rates in patients undergoing breast-conservation treatment," *Breast Cancer Res. Treat.* **163**(3), 615–622 (2017).
58. B. Z. Dashevsky et al., "The potential of high resolution magnetic resonance microscopy in the pathologic analysis of resected breast and lymph tissue," *Sci. Rep.* **5**, 17435 (2015).
59. Aspect Imaging, "M7 compact MRI," http://www.aspectimaging.com/pre-clinical-mri/aspect-one-touch-mri/m7/. (8 January 2018).
60. H. Abe et al., "Comparing post-operative human breast specimen radiograph and MRI in lesion margin and volume assessment," *J. Appl. Clin. Med. Phys.* **13**(6), 3802 (2012).
61. T. E. Doyle et al., "High-frequency ultrasound for intraoperative margin assessments in breast conservation surgery: a feasibility study," *BMC Cancer* **11**, 444 (2011).
62. M. Moschetta et al., "Role of specimen US for predicting resection margin status in breast conserving therapy," *G Chir.* **36**(5), 201–204 (2015).
63. V. Giuliano and C. Giuliano, "Improved breast cancer detection in asymptomatic women using 3D-automated breast ultrasound in mammographically dense breasts," *Clin. Imaging* **37**(3), 480–486 (2013).
64. N. C. Hall et al., "Combined approach of perioperative 18F-FDG PET/CT imaging and intraoperative 18F-FDG handheld gamma probe detection for tumor localization and verification of complete tumor resection in breast cancer," *World J. Surg. Oncol.* **5**, 143 (2007).
65. A. Chatterjee, N. Serniak, and B. J. Czerniecki, "Sentinel lymph node biopsy in breast cancer: a work in progress," *Cancer J.* **21**(1), 7–10 (2015).

66. J. E. Kalinyak et al., "Breast cancer detection using high-resolution breast PET compared to whole-body PET or PET/CT," *Eur. J. Nucl. Med. Mol. Imaging* **41**(2), 260–275 (2014).

67. D. Narayanan et al., "Interpretation of positron emission mammography and MRI by experienced breast imaging radiologists: performance and observer reproducibility," *Am. J. Roentgenol.* **196**(4), 971–981 (2011).

68. K. Schilling et al., "Positron emission mammography in breast cancer presurgical planning: comparisons with magnetic resonance imaging," *Eur. J. Nucl. Med. Mol. Imaging* **38**(1), 23–36 (2011).

69. M. R. Grootendorst et al., "Cerenkov luminescence imaging (CLI) for image-guided cancer surgery," *Clin. Transl. Imaging* **4**(5), 353–366 (2016).

70. M. R. Grootendorst et al., "Intraoperative assessment of tumor resection margins in breast-conserving surgery using (18)F-FDG cerenkov luminescence imaging: a first-in-human feasibility study," *J. Nucl. Med.* **58**(6), 891–898 (2017).

71. R. J. Halter, A. Hartov, and K. D. Paulsen, "A broadband high-frequency electrical impedance tomography system for breast imaging," *IEEE Trans. Biomed. Eng.* **55**(2Pt1), 650–659 (2008).

72. N. K. Soni et al., "Multi-frequency electrical impedance tomography of the breast: new clinical results," *Physiol. Meas.* **25**(1), 301–314 (2004).

73. T. E. Kerner et al., "Electrical impedance spectroscopy of the breast: clinical imaging results in 26 subjects," *IEEE Trans. Med. Imaging* **21**(6), 638–645 (2002).

74. K. S. Osterman et al., "Multifrequency electrical impedance imaging: preliminary in vivo experience in breast," *Physiol. Meas.* **21**(1), 99–109 (2000).

75. M. Thill, "MarginProbe: intraoperative margin assessment during breast conserving surgery by using radiofrequency spectroscopy," *Expert Rev. Med. Devices* **10**(3), 301–315 (2013).

76. T. M. Allweis et al., "A prospective, randomized, controlled, multicenter study of a real-time, intraoperative probe for positive margin detection in breast-conserving surgery," *Am. J. Surg.* **196**(4), 483–489 (2008).

77. F. Schnabel and L. Tafra, "PD02-04: a randomized, prospective, multicenter study of the impact of intraoperative margin assessment with adjunctive use of marginprobe vs. standard of care," *Cancer Res.* **71**(Suppl. 24) PD02-04 (2011).

78. M. Thill et al., "Intraoperative assessment of surgical margins during breast conserving surgery of ductal carcinoma in situ by use of radiofrequency spectroscopy," *Breast* **20**(6), 579–580 (2011).

79. F. Schnabel et al., "A randomized prospective study of lumpectomy margin assessment with use of MarginProbe in patients with nonpalpable breast malignancies," *Ann. Surg. Oncol.* **21**(5), 1589–1595 (2014).

80. J. M. Dixon et al., "Intra-operative assessment of excised breast tumour margins using ClearEdge imaging device," *Eur. J. Surg. Oncol.* **42**(12), 1834–1840 (2016).

81. G. R. Gibson et al., "A comparison of ink-directed and traditional whole-cavity re-excision for breast lumpectomy specimens with positive margins," *Ann. Surg. Oncol.* **8**(9), 693–704 (2001).

82. T. Fysh, A. Boddy, and A. Godden, "Quantifying potential error in painting breast excision specimens," *Int. J. Breast Cancer* **2013**, 1–4 (2013).

83. M. Singh et al., "The effect of intraoperative specimen inking on lumpectomy re-excision rates," *World J. Surg. Oncol.* **8**, 4 (2010).

84. D. M. McClatchy, 3rd et al., "Molecular dyes used for surgical specimen margin orientation allow for intraoperative optical assessment during breast conserving surgery," *J. Biomed. Opt.* **20**(4), 040504 (2015).

85. D. Piras et al., "Photoacoustic imaging of the breast using the twente photoacoustic mammoscope: present status and future perspectives," *IEEE J. Sel. Top. Quantum Electron.* **16**(4), 730–739 (2010).

86. R. Li et al., "Assessing breast tumor margin by multispectral photoacoustic tomography," *Biomed. Opt. Express* **6**(4), 1273–1281 (2015).

87. A. Mazhar et al., "Wavelength optimization for rapid chromophore mapping using spatial frequency domain imaging," *J. Biomed. Opt.* **15**(6), 061716 (2010).

88. A. M. Laughney et al., "Spectral discrimination of breast pathologies in situ using spatial frequency domain imaging," *Breast Cancer Res.* **15**(4), R61 (2013).

89. Q. R. J. G. Tummers et al., "Real-time intraoperative detection of breast cancer using near-infrared fluorescence imaging and methylene blue," *Eur. J. Surg. Oncol.* **40**(7), 850–858 (2014).

90. S. L. Troyan et al., "The FLARE intraoperative near-infrared fluorescence imaging system: a first-in-human clinical trial in breast cancer sentinel lymph node mapping," *Ann. Surg. Oncol.* **16**(10), 2943–2952 (2009).

91. L. E. Lamberts et al., "Tumor-specific uptake of fluorescent bevacizumab-IRDye800CW microdosing in patients with primary breast cancer: a phase I feasibility study," *Clin. Cancer Res.* **23**(11), 2730–2741 (2017).

92. M. J. Whitley et al., "A mouse-human phase 1 co-clinical trial of a protease-activated fluorescent probe for imaging cancer," *Sci. Transl. Med.* **8**(320), 320ra4 (2016).

93. S. Harmsen et al., "Optical surgical navigation for precision in tumor resections," *Mol. Imaging Biol.* **19**(3), 357–362 (2017).

94. M. D. Keller et al., "Autofluorescence and diffuse reflectance spectroscopy and spectral imaging for breast surgical margin analysis," *Lasers Surg. Med.* **42**(1), 15–23 (2010).

95. J. E. Phipps et al., "Automated detection of breast cancer in resected specimens with fluorescence lifetime imaging," *Phys. Med. Biol.* **63**(1), 015003 (2017).

96. I. J. Bigio et al., "Diagnosis of breast cancer using elastic-scattering spectroscopy: preliminary clinical results," *J. Biomed. Opt.* **5**(2), 221–228 (2000).

97. K. S. Johnson et al., "Elastic scattering spectroscopy for intraoperative determination of sentinel lymph node status in the breast," *J. Biomed. Opt.* **9**(6), 1122–1128 (2004).

98. L. G. Wilke et al., "Rapid noninvasive optical imaging of tissue composition in breast tumor margins," *Am. J. Surg.* **198**(4), 566–574 (2009).

99. C. Zhu et al., "Diagnosis of breast cancer using diffuse reflectance spectroscopy: comparison of a Monte Carlo versus partial least squares analysis based feature extraction technique," *Lasers Surg. Med.* **38**(7), 714–724 (2006).

100. R. Nachabe et al., "Diagnosis of breast cancer using diffuse optical spectroscopy from 500 to 1600 nm: comparison of classification methods," *J. Biomed. Opt.* **16**(8), 087010 (2011).

101. R. M. Levenson et al., "Slide-free histology via MUSE: UV surface excitation microscopy for imaging unsectioned tissue (conference presentation)," *Proc. SPIE* **9703**, 97030 (2016).

102. F. Fereidouni et al., "Microscopy with ultraviolet surface excitation for rapid slide-free histology," *Nat. Biomed. Eng.* **1**(12), 957–966 (2017).

103. A. K. Glaser et al., "Light-sheet microscopy for slide-free non-destructive pathology of large clinical specimens," *Nat. Biomed. Eng.* **1**, 0084 (2017).

104. J. Mertz, "Nonlinear microscopy: new techniques and applications," *Curr. Opin. Neurobiol.* **14**(5), 610–616 (2004).

105. Y. K. Tao et al., "Assessment of breast pathologies using nonlinear microscopy," *Proc. Natl. Acad. Sci. U. S. A.* **111**(43), 15304–15309 (2014).

106. T. Yoshitake et al., "Direct comparison between confocal and multiphoton microscopy for rapid histopathological evaluation of unfixed human breast tissue," *J. Biomed. Opt.* **21**(12), 126021 (2016).

107. F. T. Nguyen et al., "Intraoperative evaluation of breast tumor margins with optical coherence tomography," *Cancer Res.* **69**(22), 8790–8796 (2009).

108. S. J. Erickson-Bhatt et al., "Real-time imaging of the resection bed using a handheld probe to reduce incidence of microscopic positive margins in cancer surgery," *Cancer Res.* **75**(18), 3706–3712 (2015).

109. A. M. Zysk et al., "Intraoperative assessment of final margins with a handheld optical imaging probe during breast-conserving surgery may reduce the reoperation rate: results of a multicenter study," *Ann. Surg. Oncol.* **22**(10), 3356–3362 (2015).

110. Perimeter Medical Imaging, "The optical tissue imaging system (OTIS™)," 2018, https://www.perimetermed.com/perimeters-otistrade.html (4 July 2018).

111. A. S. Haka et al., "In vivo margin assessment during partial mastectomy breast surgery using raman spectroscopy," *Cancer Res.* **66**(6), 3317–3322 (2006).

112. M. D. Keller et al., "Development of a spatially offset Raman spectroscopy probe for breast tumor surgical margin evaluation," *J. Biomed. Opt.* **16**(7), 077006 (2011).

113. G. Thomas et al., "Evaluating feasibility of an automated 3-dimensional scanner using Raman spectroscopy for intraoperative breast margin assessment," *Sci. Rep.* **7**(1), 13548 (2017).

114. Y. W. Wang et al., "Raman-encoded molecular imaging with topically applied SERS nanoparticles for intraoperative guidance of lumpectomy," *Cancer Res.* **77**(16), 4506–4516 (2017).

Biographies for the authors are not available.